Supplementary materials

A biosynthesis pathway for 3-hydroxypropionic acid production in genetically engineered *Saccharomyces cerevisiae*

Tian Tong[a], Zhenyan Tao[b,c,d], Xiulai Chen[b,c,d], Cong Gao[b,c,d], Hui Liu[b,c,d], Gao-Qiang Liu[a,*] and Liming Liu[b,c,d,*]

[a]*Hunan Provincial Key Laboratory for Forestry Biotechnology and International Cooperation Base of Science and Technology Innovation on Forest Resource Biotechnology, Central South University of Forestry and Technology, Changsha 410004, China*

[b]*State Key Laboratory of Food Science and Technology, Jiangnan University, Wuxi 214122, China*

[c]*Key Laboratory of Industrial Biotechnology, Ministry of Education, Jiangnan University, Wuxi 214122, China*

[d]*International Joint Laboratory on Food Safety, Jiangnan University, Wuxi 214122, China*

*Corresponding author: Hunan Provincial Key Laboratory for Forestry Biotechnology, Central South University of Forestry and Technology, 498 South Shaoshan Road, Changsha 410004, China. *E-mail address*: gaoliuedu@csuft.edu.cn (Gao-Qiang Liu).

State Key Laboratory of Food Science and Technology, Jiangnan University, 1800 Lihu Road, Wuxi 214122, China. *E-mail address*: mingll@jiangnan.edu.cn (Liming Liu).

This file includes:

Supplementary Fig. 1 to Supplementary Fig. 12

Supplementary Table 1 to Supplementary Table 5

Supplementary Note 1 to Supplementary Note 5

Supplementary Experimental 1 to Supplementary Experimental 8

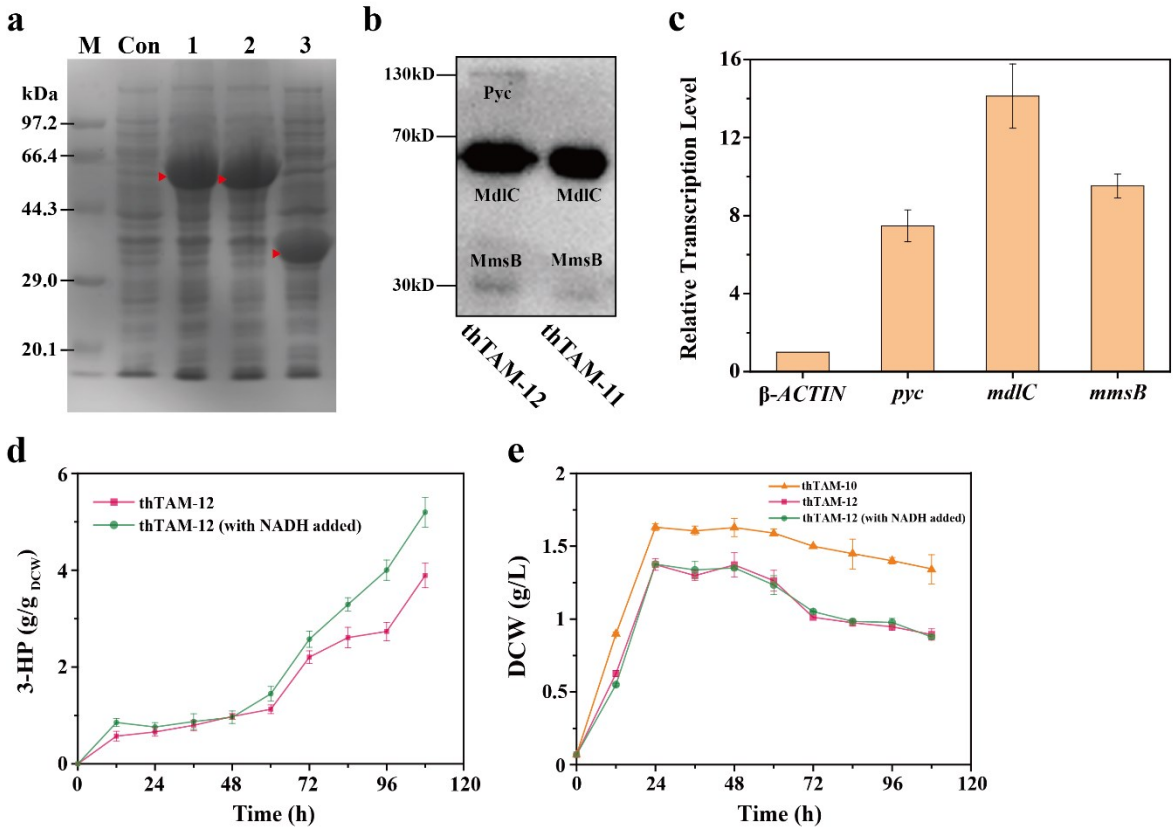

Fig. 1. (**a**) The SDS-PAGE verifies the enzymes expression in *E. coli* BL21-2, BL21-3, and BL21-4. M, represents protein standard molecular weight marker; Con, represents protein in control strain BL21-1 (harboring an empty plasmid pET28a); Lane 1, represents protein in strain BL21-2 (harboring pET28a-*kdcA*); Lane 2, represents protein in strain BL21-3 (harboring pET28a-*mdlC*); Lane 3, represents protein in strain BL21-4 (harboring pET28a-*mmsB*). Since protein expressed by plasmid pET28a respectively introduces His tag and spacer amino acids at the C- and N-terminal, the expected sizes of overexpressed proteins are: KdcA, 60.9 kDa; MdlC, 61.0 kDa; MmsB, 35.9 kDa. (**b**) Western blot analysis of strains thTAM-12 (strain thTAM overexpressing genes *pyc*, *mdlC*, and *mmsB*. Pyc, 131.2 kDa; MdlC, 56.4 kDa; MmsB, 30.3 kDa) and thTAM-11 (strain thTAM overexpressing genes *mdlC* and *mmsB*). (**c**) Relative transcriptional levels of genes *pyc*, *mdlC*, and *mmsB* in the strain thTAM-12. The β-*ACTIN* gene was used as the internal control. (**d**) 3-HP yield by strains thTAM-12 and thTAM-12 with NADH added in shake-flask cultivation. (**e**) DCW of strains thTAM-10, thTAM-12, and thTAM-12 with NADH added.

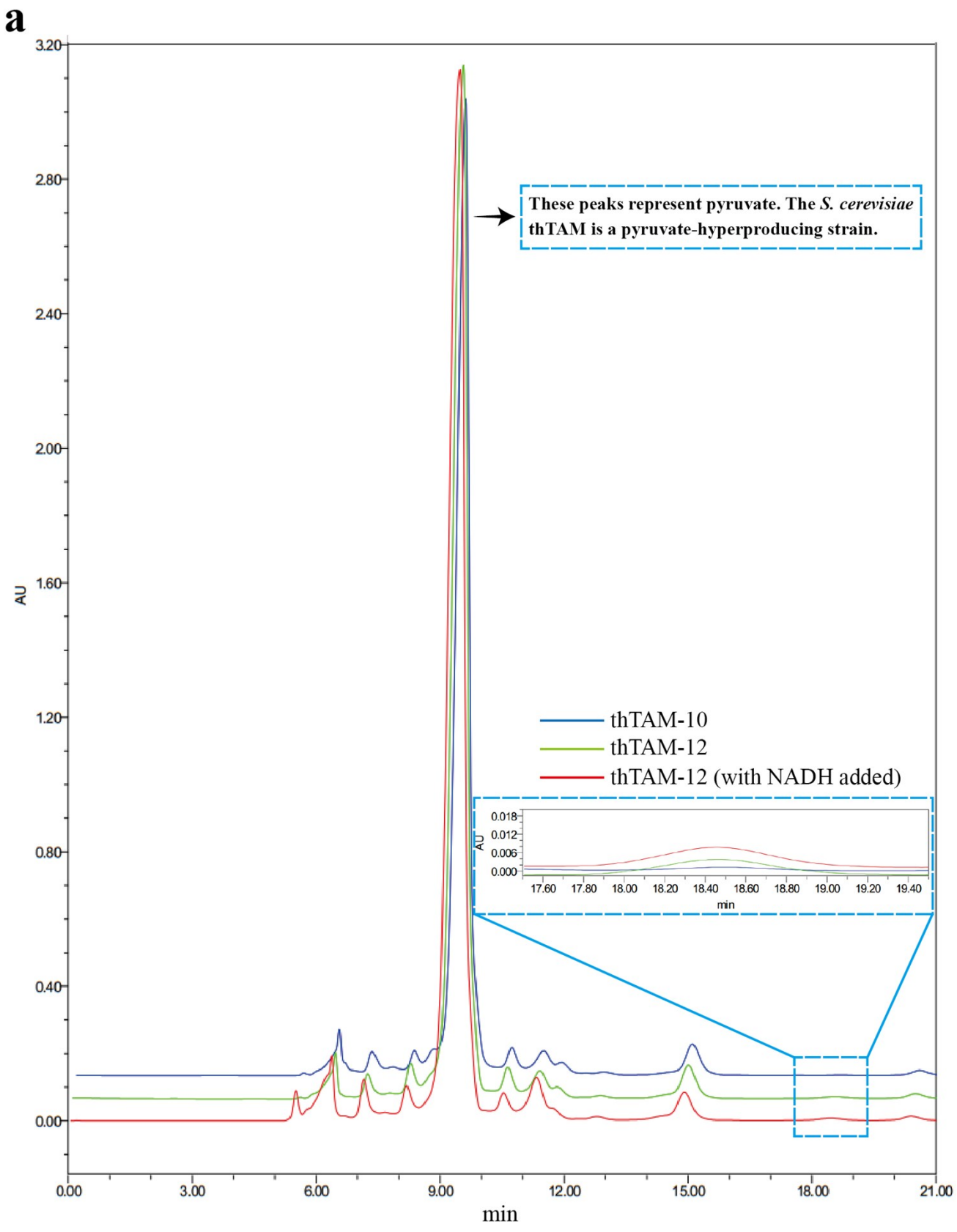
a
These peaks represent pyruvate. The S. cerevisiae thTAM is a pyruvate-hyperproducing strain.
thTAM-10
thTAM-12
thTAM-12 (with NADH added)
AU
min
3.20
2.80
2.40
2.00
1.60
1.20
0.80
0.40
0.00
0.00
3.00
6.00
9.00
12.00
15.00
18.00
21.00
0.018
0.012
0.006
0.000
17.60
17.80
18.00
18.20
18.40
18.60
18.80
19.00
19.20
19.40

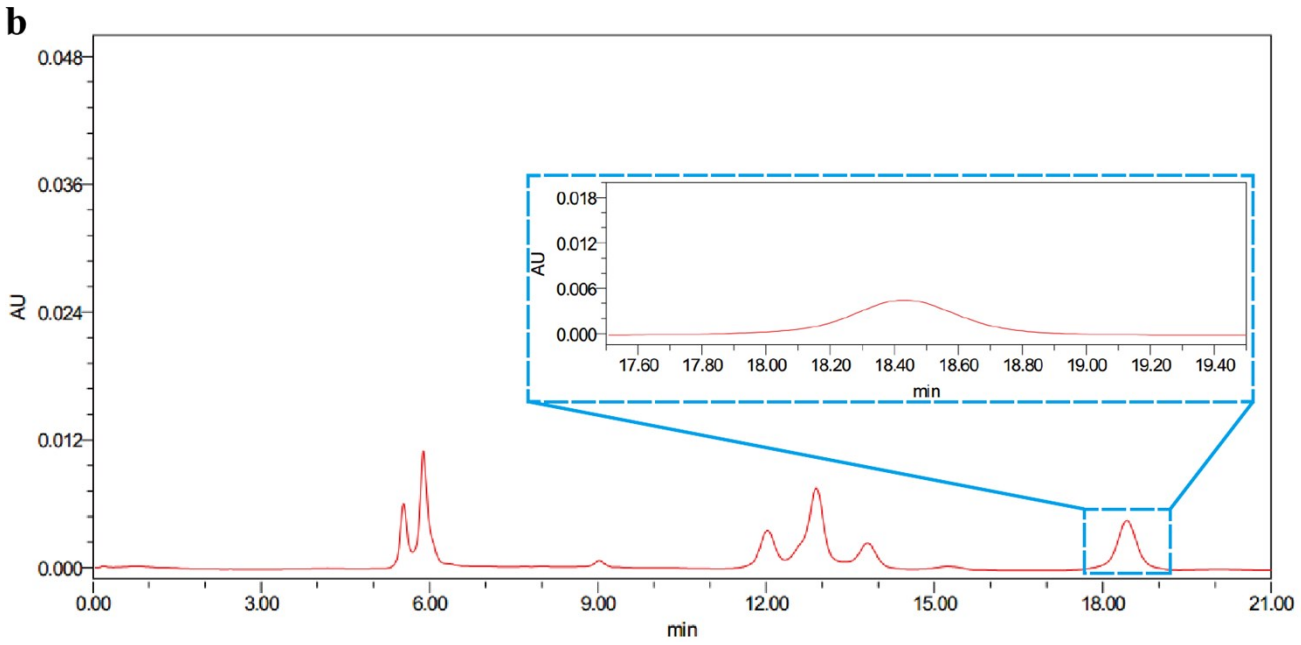

Fig. 2. (**a**) 3-HP production analysis by HPLC in shake-flask cultivation at 108 h. Peaks with retention times of 18.43 min represent 3-HP. (**b**) Red solid lines represent 1g/L 3-HP (> 95%) analysis by HPLC. Peaks with retention times of 18.43 min represent 3-HP.

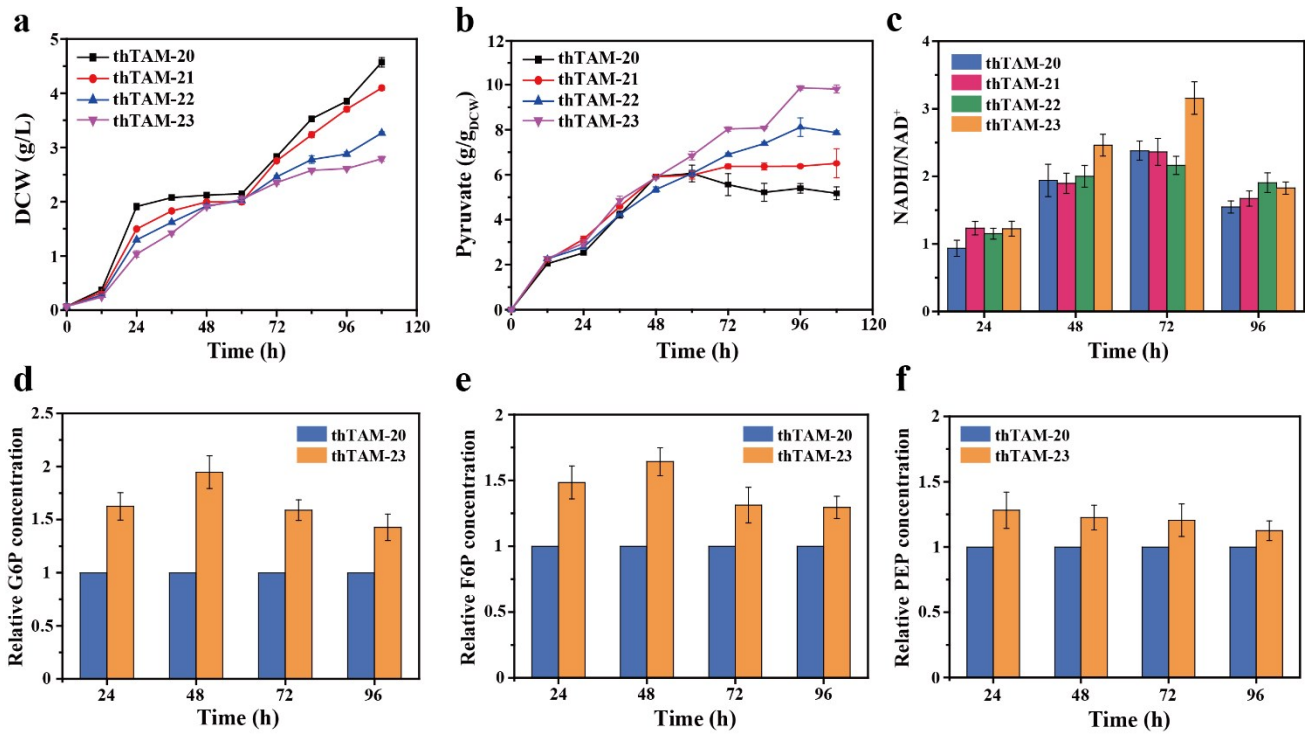

Fig. 3. (**a**) Dry cell weight (DCW) of strains thTAM-20, thTAM-21, thTAM-22, and thTAM-23 in shake-flask cultivation. (**b**) Pyruvate yield of the four strains in shake-flask cultivation. (**c**) Ratio of intracellular NADH/NAD$^+$ in the four strains. (**d**) Relative intracellular concentration of glucose-6-phosphate (G6P) in strain thTAM-20 and thTAM-23. (**e**) Relative intracellular concentration of fructose-6-phosphate (F6P) in strain thTAM-20 and thTAM-23. (**f**) Relative intracellular concentration of phosphoenolpyruvate (PEP) in strain thTAM-20 and thTAM-23.

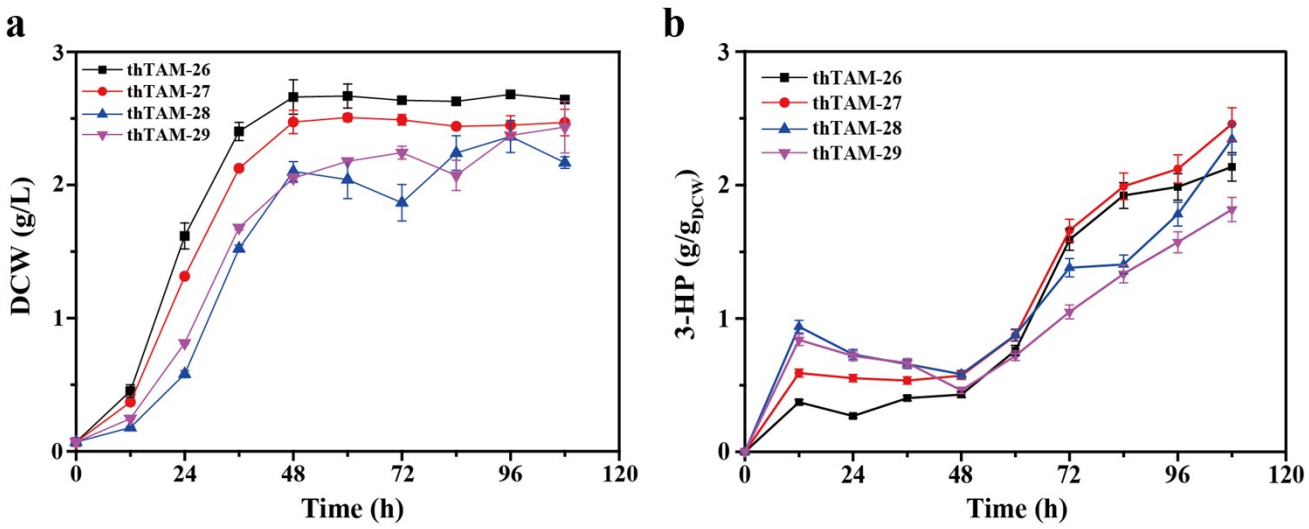

Fig. 4. (**a**) DCW of strains thTAM-26, thTAM-27, thTAM-28, and thTAM-29 in shake-flask cultivation. (**b**) 3-HP yield by strains thTAM-26, thTAM-27, thTAM-28, and thTAM-29 in shake-flask cultivation.

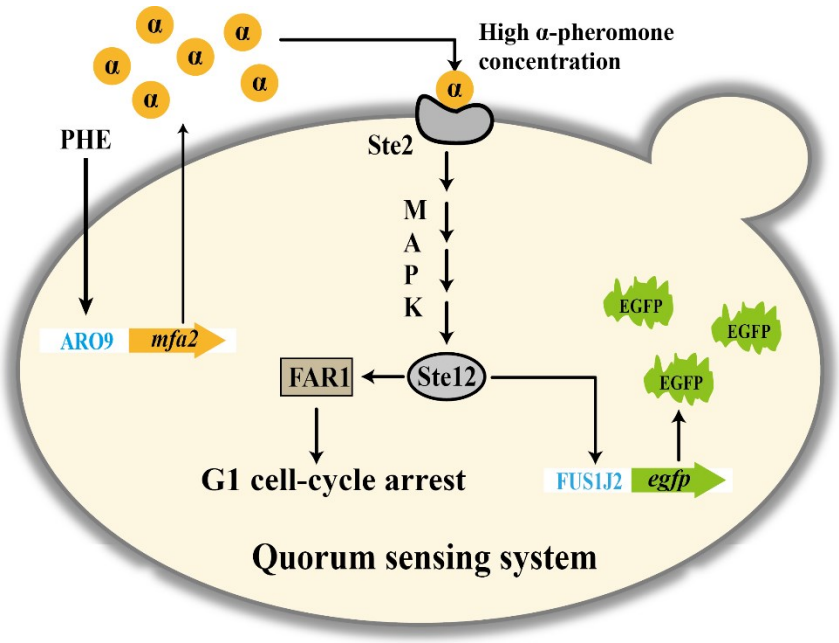

Fig. 5. Schematic diagram of phenylalanine (PHE) responsive the quorum-sensing circuit. This circuit was constructed in a *bar1* (α-pheromone protease gene) deletion genetic background, which is required to avoid signal degradation. The *ARO9* promoter is PHE responsive promoter, and controls the expression of the α-pheromone gene *mfα2*. When cells grow to a high population density, the extracellular α-pheromone binds to mating-type-specific membrane receptors Ste2 at a threshold concentration to trigger the FAR1 protein and the *FUS1J2* promoter via the intracellular MAPK signaling cascade, causing cells to arrest growth in the G1 phase of the cell cycle and the EGFP reporter expression.

To test the validity of the *ARO9* promoter in strain thTAM, strain thTAM-34 (harboring the plasmid YEplac112-pARO9-EGFP) was produced and grown with 0, 100, 200, 300, and 400 μg/mL of PHE, respectively, we found that 100 μg/mL of PHE could activate the *ARO9* promoter to express the EGFP.

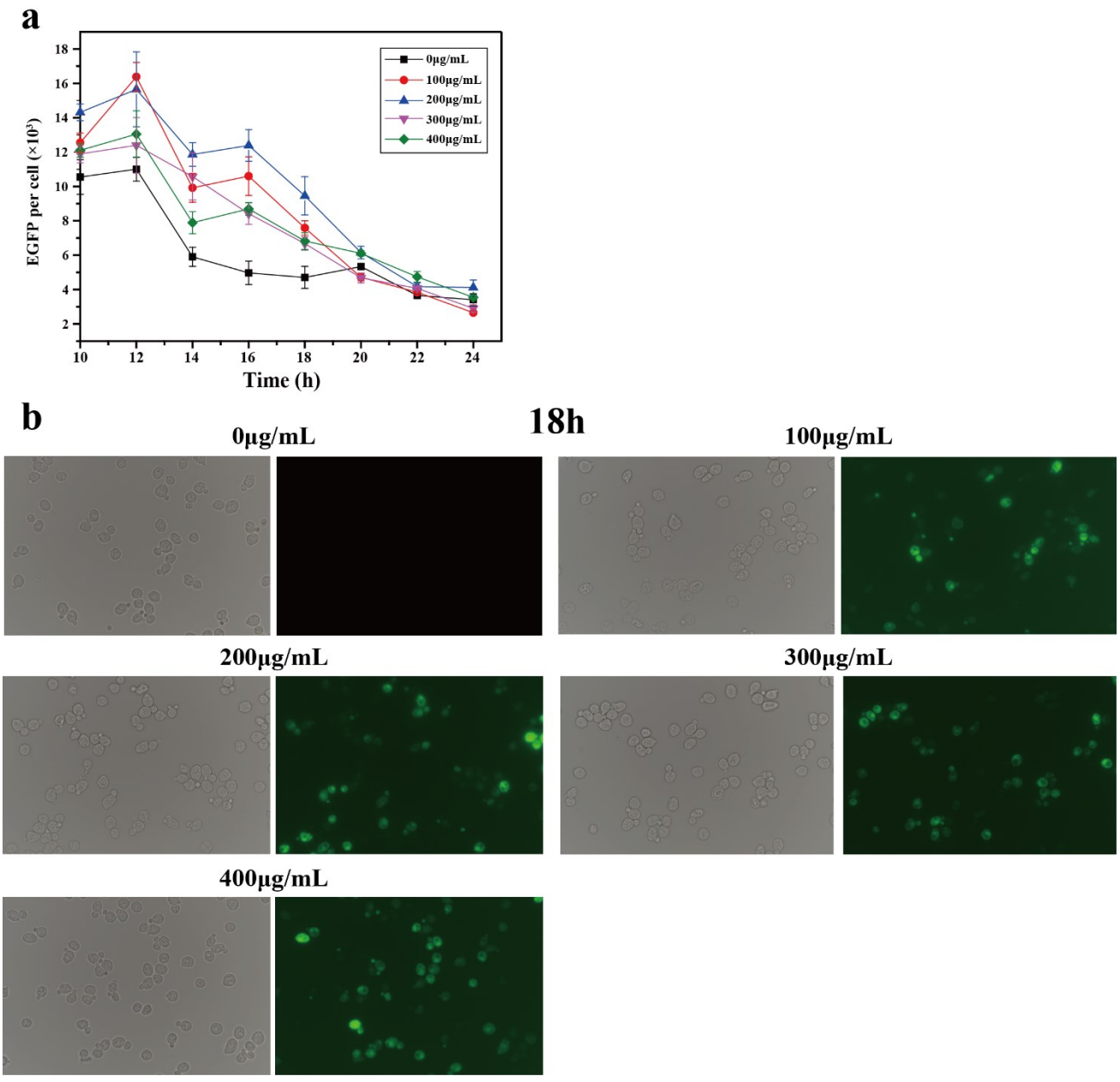

Fig. 6. (**a**) EGFP per cell of strain thTAM-34 in medium with different concentrations of PHE during 10 h to 24 h. (**b**) Light microscopy images of cell morphology and fluorescence microscope images of the EGFP expression of strain thTAM-34 after add various concentrations of PHE at 18 h.

Strain thTAM-35 (harboring the plasmid YEplac112-pFUS1J2-EGFP) was used to detect the availability of the *FUS1J2* promoter. The *α*-pheromone with concentrations of 0, 1, 2.5, 5, 10, and 25 μmol/L were respectively added when strain thTAM-35 was growing to the mid-logarithmic phase (at 20 h) to induce the EGFP expression. The observed results indicated that 1 μmol/L of *α*-pheromone could activate the *FUS1J2* promoter to express the EGFP.

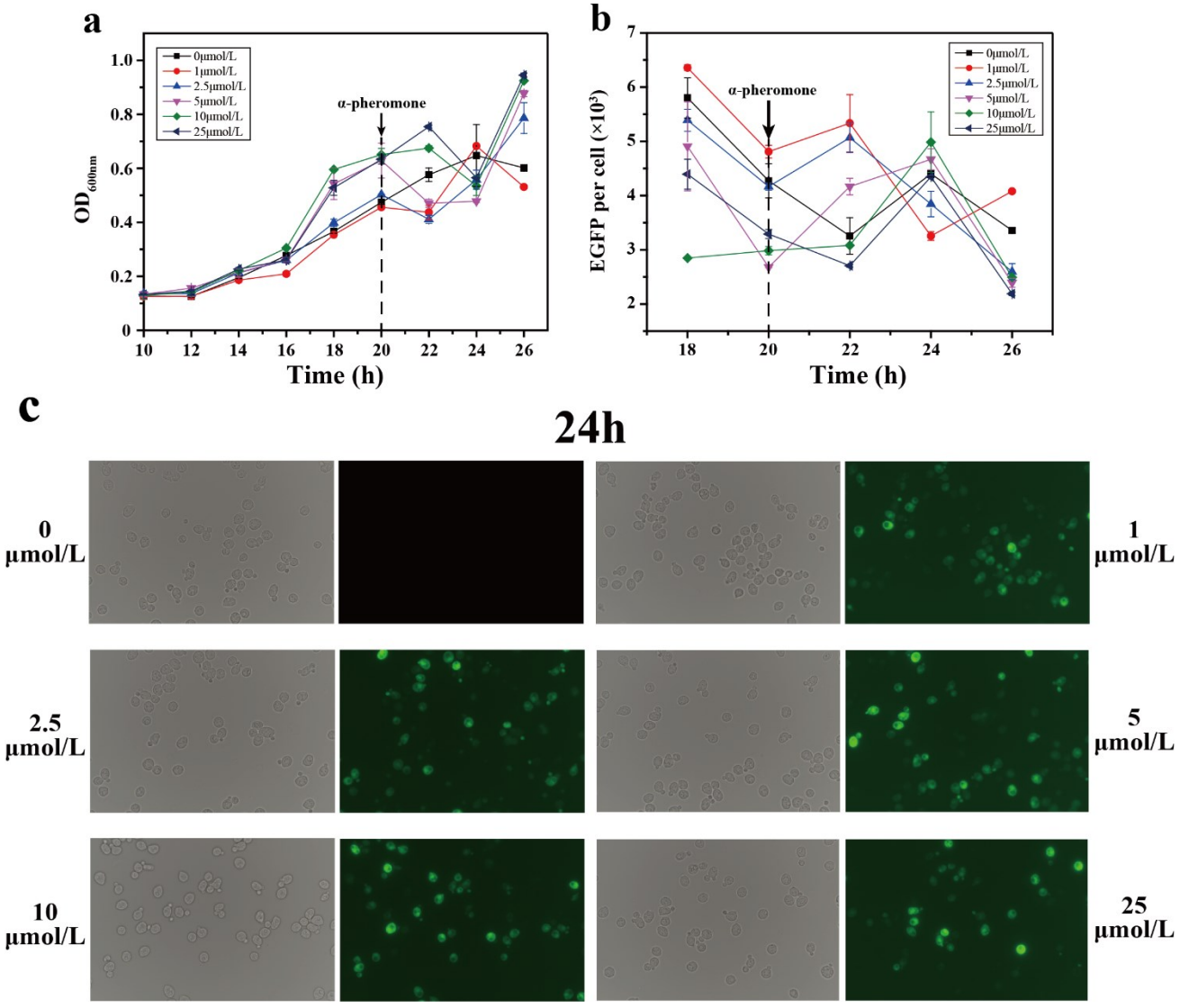

Fig. 7. (**a**) OD_{600nm} of strain thTAM-35 in medium that add different concentrations of α-pheromone at 20 h. (**b**) EGFP per cell of strain thTAM-35 in medium with different concentrations of α-pheromone during 18 h to 26 h. (**c**) Light microscopy images of cell morphology and fluorescence microscope images of the EGFP expression of the strain thTAM-35 at 24 h.

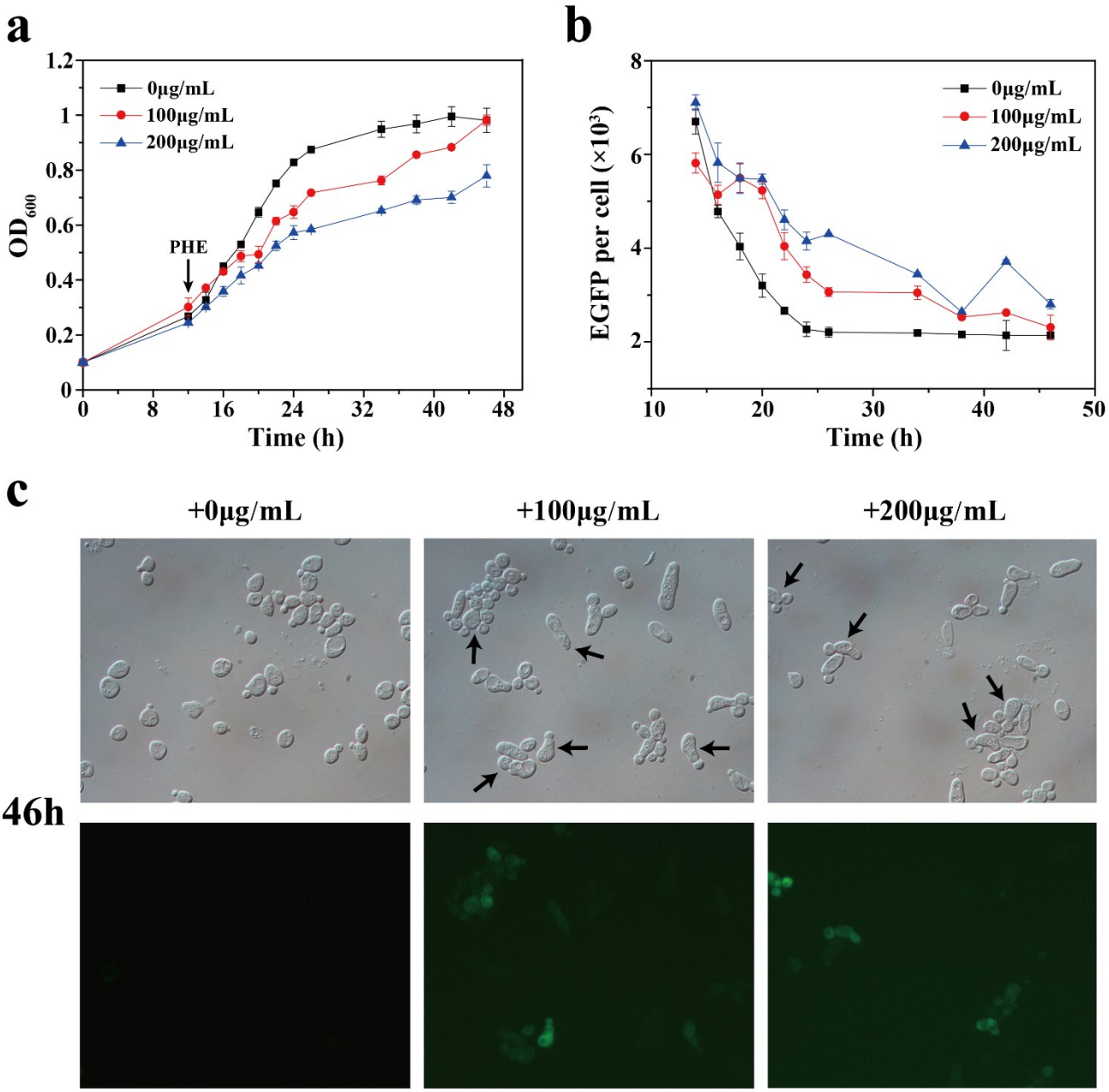

Fig. 8. (**a**) Growth of strain thTAM-36-1 in medium with different concentrations of PHE. (**b**) EGFP per cell of strain thTAM-36-1 in medium with different concentrations of PHE during 12 h to 46 h. (**c**) Light microscopy images of "shmoo" cell morphology (black arrow mark) and fluorescence microscope images of the EGFP expression of strain thTAM-36-1 after the QS system was fully activated at 46 h. Simultaneously, the cells mated, as determined by a pear shaped "shmoo" cell morphology.

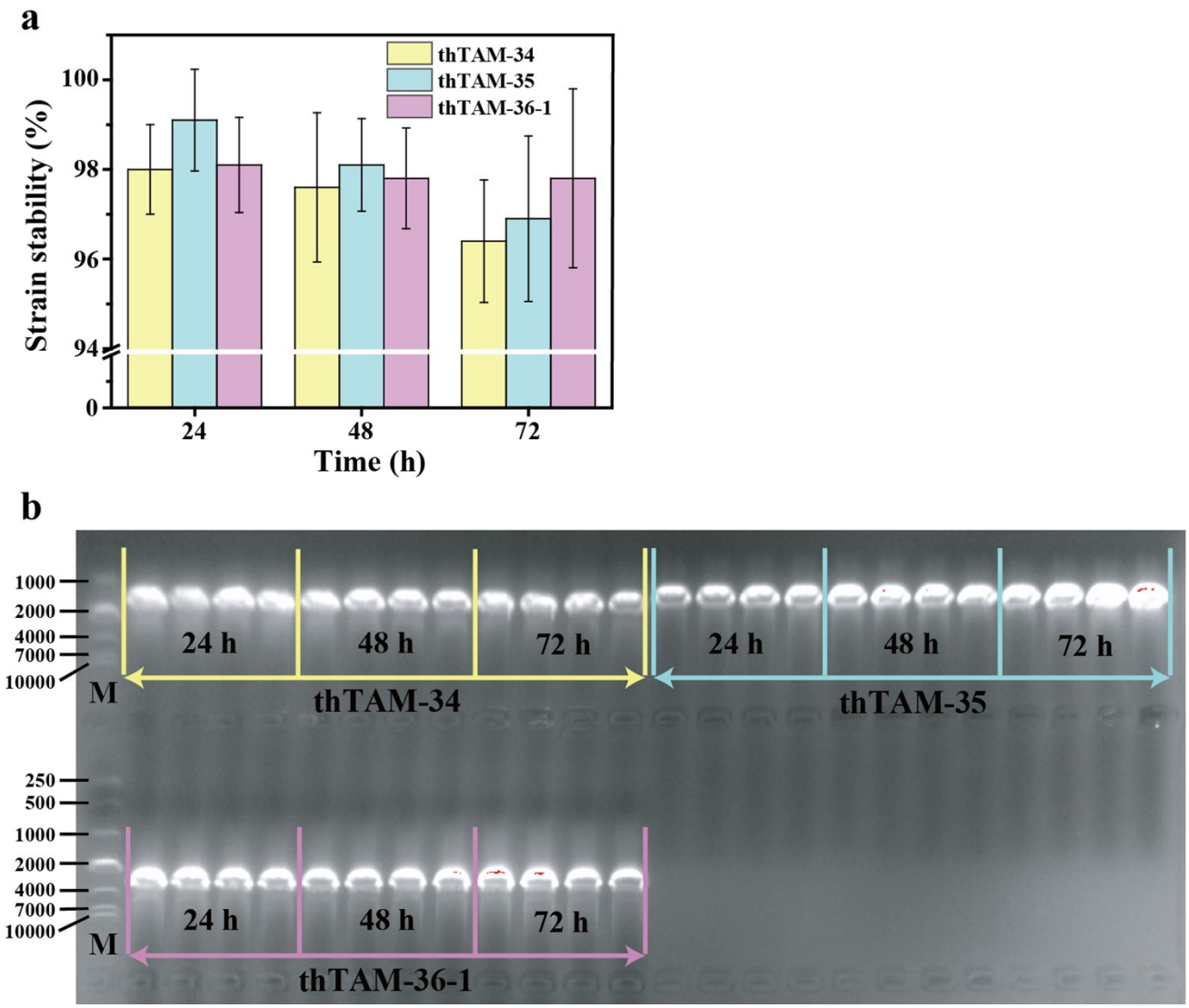

Fig. 9. (**a**) Analysis of strain stability by colony count of strains thTAM-34, thTAM-35, and thTAM-36-1 within different cultivation time. (**b**) Gel image of PCR product amplified using plasmids DNA extracted from four randomly picked single colony of strains thTAM-34, thTAM-35, and thTAM-36-1 within different cultivation time as a template. The lengths of corresponding DNA fragment are 1574 bp (yellow area), 1360 bp (blue area), and 2723 bp (purple area), respectively. M, represents DNA Marker (DL 10,000 DNA Marker, Takara Bio).

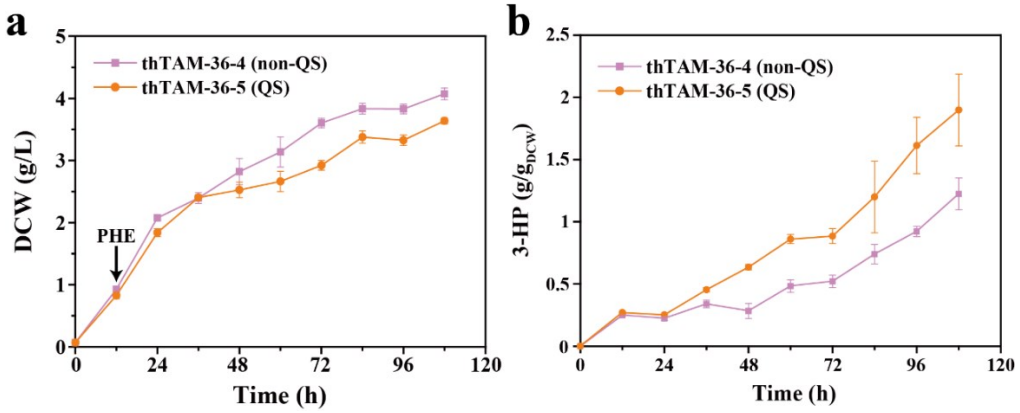

136

137 **Fig. 10.** (**a**) DCW of strains thTAM-36-4 (non-QS) and thTAM-36-5 (QS) in shake-flask cultivation. (**b**) 3-HP yield

138 by strains thTAM-36-4 (non-QS) and thTAM-36-5 (QS) in shake-flask cultivation.

139

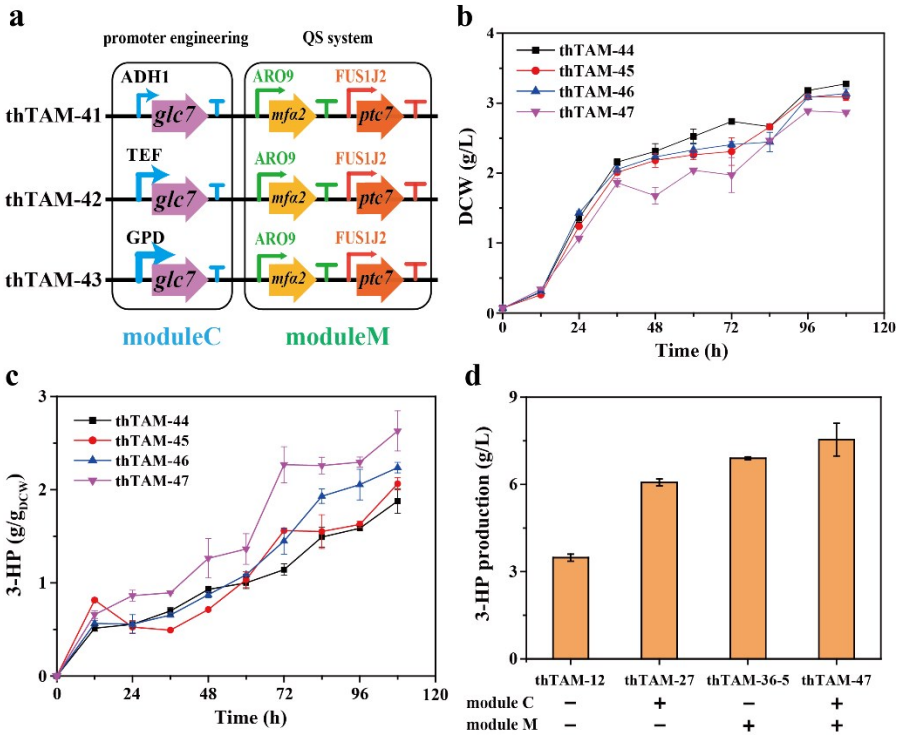

140

141 **Fig. 11.** (**a**) Dynamic dephosphorylation regulation was achieved through the assembly of *glc7* and *ptc7* expression

142 cassettes. Module C, cytoplasmic energy module; module M, mitochondria energy module. (**b**) DCW of strains

143 thTAM-44, thTAM-45, thTAM-46, and thTAM-47 in shake-flask cultivation. (**c**) 3-HP yield by strains thTAM-44,

144 thTAM-45, thTAM-46, and thTAM-47 in shake-flask cultivation. (**d**) 3-HP production comparison for strains

145 thTAM-12, thTAM-27, thTAM-36-5, and thTAM-47.

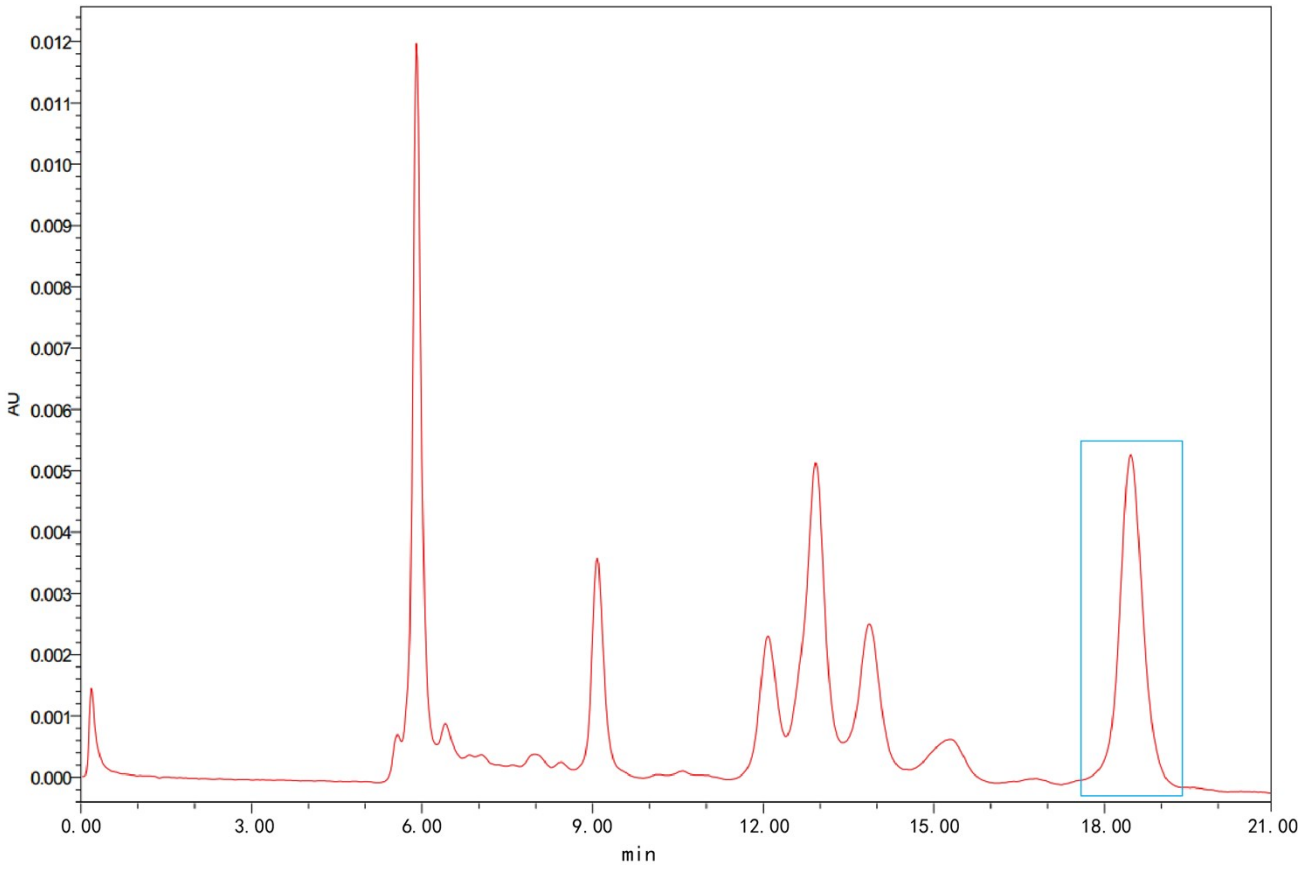

Fig. 12. Yield analysis of 3-HP isolated from fermentation broth by HPLC after 500-fold dilution. Peaks with retention times of 18.43 min represent 1.195 g/L 3-HP.

159 **Table 1.** Strains used in this study

Strains	Description	Source
E.*coli* BL21(DE3)	For enzyme expression and purification	Novagen
BL21-1	E. *coli* BL21(DE3)+pET28a	This study
BL21-2	E. *coli* BL21(DE3)+pET28a/T7-*kdcA*	This study
BL21-3	E. *coli* BL21(DE3)+pET28a/T7-*mdlC*	This study
BL21-4	E. *coli* BL21(DE3)+pET28a/T7-*mmsB*	This study
TAM	MTAa *pdc1(-6,-2)*::*loxp pdc5(-6,-2)*::*loxp pdc6(-6,-2)*::*loxp ura3*-52, C2-independent, glucose-tolerant, and pyruvate-hyperproducing yeast	Lab collection
thTAM	TAM *TRP1*::loxp *HIS3*::loxp	This study
thTAM-10	thTAM+pY26	This study
thTAM-11	thTAM+pY26/TEF-*mmsB* GPD-*mdlC*	This study
thTAM-12	thTAM+pY26/TEF-*mmsB* GPD-*mdlC* GPD-*pyc*	This study
thTAM-20	thTAM+pY14	This study
thTAM-21	thTAM+pY14/ADH1-*cdc28*	This study
thTAM-22	thTAM+pY14/ADH1-*gcr2*	This study
thTAM-23	thTAM+pY14/ADH1-*glc7*	This study
thTAM-24	thTAM+pY26/GPD-*hxk2*	This study
thTAM-25	thTAM+pY26/TEF-*glc7* GPD-*hxk2*	This study
thTAM-26	thTAM+YEplac112 pY26/TEF-*mmsB* GPD-*mdlC* GPD-*pyc*	This study
thTAM-27	thTAM+YEplac112/ADH1-*glc7* pY26/TEF-*mmsB* GPD-*mdlC* GPD-*pyc*	This study
thTAM-28	thTAM+YEplac112/TEF-*glc7* pY26/TEF-*mmsB* GPD-*mdlC* GPD-*pyc*	This study
thTAM-29	thTAM+YEplac112/GPD-*glc7* pY26/TEF-*mmsB* GPD-*mdlC* GPD-*pyc*	This study
thTAM-30	thTAM+ YEplac112	This study
thTAM-31	thTAM+ YEplac112/ADH1-*ptc5*	This study
thTAM-32	thTAM+ YEplac112/ADH1-*ptc7*	This study
thTAM-33	thTAM+ YEplac112/ADH1-*smk1*	This study
thTAM-34	thTAM+YEplac112/ARO9-*EGFP*	This study
thTAM-35	thTAM+YEplac112/FUS1J2-*EGFP*	This study
thTAM-36	thTAM *bar1*Δ	This study
thTAM-36-1	thTAM+YEplac112/ARO9-*mfα2* FUS1J2-*EGFP bar1*Δ	This study
thTAM-36-2	thTAM+YEplac112 *bar1*Δ	This study
thTAM-36-3	thTAM+YEplac112/ARO9-*mfα2* FUS1J2-*ptc7 bar1*Δ	This study
thTAM-36-4	thTAM+YEplac112 pY26/TEF-*mmsB* GPD-*mdlC* GPD-*pyc bar1*Δ	This study
thTAM-36-5	thTAM+YEplac112/ARO9-*mfα2* FUS1J2-*ptc7* pY26/TEF-*mmsB* GPD-*mdlC* GPD-*pyc bar1*Δ	This study
thTAM-40	thTAM+YEplac112 *bar1*Δ	This study
thTAM-41	thTAM+YEplac112/ADH1-*glc7* ARO9-*mfα2* FUS1J2-*ptc7 bar1*Δ	This study
thTAM-42	thTAM+YEplac112/TEF-*glc7* ARO9-*mfα2* FUS1J2-*ptc7 bar1*Δ	This study
thTAM-43	thTAM+YEplac112/GPD-*glc7* ARO9-*mfα2* FUS1J2-*ptc7 bar1*Δ	This study
thTAM-44	thTAM+YEplac112 pY26/TEF-*mmsB* GPD-*mdlC* GPD-*pyc bar1*Δ	This study
thTAM-45	thTAM+YEplac112/ADH1-*glc7* ARO9-*mfα2* FUS1J2-*ptc7* pY26/TEF-	This study

	mmsB GPD-*mdlC* GPD-*pyc bar1*Δ	
thTAM-46	thTAM+YEplac112/TEF-*glc7* ARO9-*mfα2* FUS1J2-*ptc7* pY26/TEF-*mmsB* GPD-*mdlC* GPD-*pyc bar1*Δ	This study
thTAM-47	thTAM+YEplac112/GPD-*glc7* ARO9-*mfα2* FUS1J2-*ptc7* pY26/TEF-*mmsB* GPD-*mdlC* GPD-*pyc bar1*Δ	This study

186 **Table 2.** Plasmids constructed in this study

Plasmids	Description	Source
YEplac112	Amp, TRP1, 2μ ori	YouBio
pY14	Amp, TRP1, CEN/ARS	Turbo
pY26	URA3, 2μ ori	Turbo
pML104	Amp, URA3, 2μ ori	Turbo
pY26/TEF-*mmsB* GPD-*mdlC*	URA3, 2μ ori, $P_{TEF,\ GPD}$, overexpression *mmsB*, *mdlC*	This study
pY26/TEF-*mmsB* GPD-*mdlC* GPD-*pyc*	URA3, 2μ ori, $P_{TEF,\ GPD}$, overexpression *mmsB*, *mdlC*, *pyc*	This study
pY26/GPD-*hxk2*	URA3, 2μ ori, P_{GPD}, overexpression *hxk2*	This study
pY26/TEF-*glc7* GPD-*hxk2*	URA3, 2μ ori, $P_{TEF,\ GPD}$, overexpression *glc7*, *hxk2*	This study
pY14/ADH1-*glc7*	TRP1, CEN/ARS, P_{ADH1}, overexpression *glc7*	This study
pY14/ADH1-*cdc28*	TRP1, CEN/ARS, P_{ADH1}, overexpression *cdc28*	This study
pY14/ADH1-*gcr2*	TRP1, CEN/ARS, P_{ADH1}, overexpression *gcr2*	This study
YEplac112/ADH1-*glc7*	TRP1, 2μ ori, P_{ADH1}, overexpression *glc7*	This study
YEplac112/TEF-*glc7*	TRP1, 2μ ori, P_{TEF}, overexpression *glc7*	This study
YEplac112/GPD-*glc7*	TRP1, 2μ ori, P_{GPD}, overexpression *glc7*	This study
YEplac112/ADH1-*ptc5*	URA3, 2μ ori, P_{GPD}, overexpression *ptc5*	This study
YEplac112/ADH1-*ptc7*	URA3, 2μ ori, P_{GPD}, overexpression *ptc7*	This study
YEplac112/ADH1-*smk1*	URA3, 2μ ori, P_{GPD}, overexpression *smk1*	This study
pML104-N20(*bar1*)	Amp, URA3, 2μ ori, $P_{TDH3,\ SNR52}$, expression *Cas9*, *gRNA*	This study
YEplac112/ARO9-EGFP	TRP1, 2μ ori, P_{ARO9}, expression *egfp*	This study
YEplac112/FUS1J2-EGFP	TRP1, 2μ ori, P_{FUS1J2}, expression *egfp*	This study
YEplac112/ARO9-*mfα2* FUS1J2-EGFP	TRP1, 2μ ori, $P_{ARO9,\ FUS1J2}$, expression *mfα2, egfp*	This study
YEplac112/ARO9-*mfα2* FUS1J2-*ptc7*	TRP1, 2μ ori, $P_{ARO9,\ FUS1J2}$, expression *mfα2, ptc7*	This study
YEplac112/ADH1-glc7 ARO9-*mfα2* FUS1J2-*ptc7*	TRP1, 2μ ori, $P_{ADH1,\ ARO9,\ FUS1J2,}$ expression *glc7*, *mfα2, ptc7*	This study
YEplac112/TEF-*glc7* ARO9-*mfα2* FUS1J2-*ptc7*	TRP1, 2μ ori, $P_{TEF,\ ARO9,\ FUS1J2}$, expression *glc7*, *mfα2, ptc7*	This study
YEplac112/GPD-*glc7* ARO9-*mfα2* FUS1J2-*ptc7*	TRP1, 2μ ori, $P_{GPD,\ ARO9,\ FUS1J2}$, expression *glc7*, *mfα2, ptc7*	This study

187

188

189

190

191

192

193

194 **Table 3.** Primers used in this study for gene cloning and plasmid construction

Primer	**Sequence (5'→3')**
KZ-*mmsB*-S	agaattgttaattaaagatctAATATCCTTCTTGCGATAACCCTC
KZ-*mmsB*-A	ttttctagaactagcgcggccgcATGCGTATCGCATTCATCGG
KZ-*pyc*-S	gacggattctagaactagtggatccATGGCGGCTCCGTTTCGTCAGCCTG
KZ-*pyc*-A	aatgtaagcgtgacataaccccgggTTACGCTTTGACGATCTTGCAGACG
KZ-*mdlC*-S	cccccgggctgcaggaattcATGAAGACCGTTCACGGTGC
KZ-*mdlC*-A	aggtcgacggtatcgataagcttAATTGGCTCGATGGTCTGAG
KZ-pADH1-S	cttgcatgcctgcaggtcgacATCCTTTTGTTGTTTCCGGGT
KZ-pADH1-A	ggtgatgcatAGTTGATTGTATGCTTGGTATAGCTTG
KZ-*cdc28*-S	ATGAGCGGTGAATTAGCAAATTAC
KZ-*cdc28*-A	TTATGATTCTTGGAAGTAGGGGTGGAT
KZ-*gcr2*-S	ATGCATCACCAAACTAAGTTAGAT
KZ-*gcr2*-A	TCATCTTTGTAAATCCCTTAACATACT
KZ-*glc7*-S	ATGGACTCACAACCAGTTGACGT
KZ-*glc7*-A	TTTTTTCTTTCTACCCCCAGCTTGCCT
KZ-*ptc5*-S	ATGTCTCCCTTAACTAGAACCGTAGCT
KZ-*ptc5*-A	TCATAATCTAGGTTTTGGCTTTGTT
KZ-*ptc7*-S	ATGTTTGCAAACGTTGGATTTAGA
KZ-*ptc7*-A	TTAGTCAACTCTCACGACAACAAC
KZ-*smk1*-S	ATGAATTGCACACTTACAGATAATACCA
KZ-*smk1*-A	CTATAAAGACGAGGAGGACAAATCGGTTTT
KZ-pARO9-S	GTTGCCGCGTGGAGACATC
KZ-pARO9-A	CTGAGTCGATGAGAGAGTGTAATTG
KZ-*mfα2*-S	ATGAAATTCATTTCTACCTTTCTCAC
KZ-*mfα2*-A	TCAGTACATTGGTTGGCCTGGCT
KZ-pFUS1J2-S	GCCCTCCTTCAATTTTTCTGG
KZ-pFUS1J2-A	TTTGATTTTCAGAAACTTGTTGGC
N20(*bar1*)-S	CTAGCTCTAAAACGCGATCCAAGTGTAGCAGAG
N20(*bar1*)-A	GATCCTCTGCTACACTTGGATCGCGTTTTAGAGCTAG
KZ-QCK-S	ATGAGTCCTTAAGAAGGCCGTTGAA
KZ-QCK-A	ATTGTATAGAATATGAATCATACTA
M13R(-48)	AGCGGATAACAATTTCACACAGGA
M13F(-47)	CGCCAGGGTTTTCCCAGTCACGAC
YZ-PY26-GPD-S	ACAAGGCAATTGACCCACG
YZ-PY26-GPD-A	ACCGGCCGCAAATTAAAGC
YZ-PY26-TEF-S	ATTTCTGGCAAGGTAGACAAGC
YZ-PY26-TEF-A	TAAAAATTTTTATCACGTTTC

195 Note: Sequences in blue indicated the homologous sequences.

196

197 **Table 4.** Different studies carried out for the production of 3-HP

Engineered strain	Biosynthesis pathway	Carbon source	Culture conditions	Glucose input (g/L)[a]	3-HP output (g/L)[b]	3-HP yield (g/g)[c]	3-HP productivity (g/L/h)	Ref
E. coli	Malonyl-CoA pathway	Glucose	Shake flask culture (10 mL in 250 mL flask)	/[d]	0.2	/	0.01	[1]
			Fed-batch, 5L bioreactor	/	40.6	0.19	0.56	[2]
			Fed-batch, 5L bioreactor	/	10.08	/	0.28	[3]
			Fed-batch, bioreactor	/	48.4	0.53	0.23	[4]
		Glucose + malonate	Shake flask culture (50 mL in 250 mL flask)	/	1.20	/	/	[5]
	Glycerol pathway	Glucose + glycerol	Fed-batch, 5L bioreactor	/	71.9	/	1.8	[6]
	β-alanine pathway	Glucose	Fed-batch, 6.6L bioreactor	/	31.1	0.423	0.63	[7]
S. cerevisiae	Malonyl-CoA pathway	Glucose	Shake flask culture (20 mL in 100 mL flask)	/	0.463	/	0.0064	[8]
			Shake flask culture	/	0.477	/	0.008	[9]
			Fed-batch, bioreactor	/	0.8	/	0.03	[10]
			Fed-batch, 1L bioreactor	/	9.8	0.07	0.1	[11]
			Fed-batch, 1L bioreactor	/	0.279	/	0.0056	[12]
	β-alanine pathway	Glucose	Fed-batch, 1L bioreactor	/	13.7	0.14	0.17	[13]

	Oxaloacetate pathway	Glucose	Fed-batch, 5L bioreactor	145	18.1	0.125	0.17	This study
Schizosaccharomyces pombe	Malonyl-CoA pathway	Glucose	Fed-batch, 1L bioreactor	/	11.4	0.112	0.12	[14]
Corynebacterium glutamicum	Glycerol pathway	Glucose + xylose	Fed-batch, 5L bioreactor	/	62.6	0.51	0.87	[15]

Note: [a] The glucose consumption (g/L) in fermentation.

[b] The 3-HP production (g/L) in fermentation.

[c] The 3-HP yield (g 3-HP/g Glucose).

[d] The value could not be calculated from given data.

Table 5. The cost of several reagents needed for the expression in fed-batch fermentation

Reagent	Price ($/g)	Consumption	Cost ($)
Biotin	4.6	1.0 mg/L*3 L= 0.003 g	0.014
Thiamine	0.27	1.6 mg/L*3 L= 0.0048 g	0.0013
Thiamine diphosphate (ThDP)	24.5	2.0 mg/L*3 L= 0.006 g	0.147
Phenylalanine (PHE)	0.66	100 mg/L*3 L= 0.3 g	0.198

Note: the price of reagent was provided by Sinopharm Chemical Reagent Co., Ltd (http://www.sinoreagent.com/) and Sangon Biotech Co., Ltd (http://www.sangon.com/product).

Supplementary Note 1.

The principle of NADH/NAD^+ and ATP assay

NADH/NAD^+ assay:

The determination of the total amount of NAD^+ and NADH is based on the oxidation of ethanol under the action of alcohol dehydrogenase and the reduction of NAD^+ to NADH. The generated NADH reduces WST-8 to orange yellow formazan under the action of electron coupling agent 1-mPMS. The maximum absorption peak of formazan is about 450 nm. The formazan produced in the reaction system is proportional to the total amount of NAD and NADH in the sample. The amount of NADH is determined by heating the sample in a 60 °C water bath for 30 min, the NAD^+ in the sample is decomposed and only NADH is retained. NADH reduces WST-8 to formazan, thereby determining the amount of NADH in the sample by colorimetry. All reagents are provided by the Kit. According to the total amount of NAD^+ and NADH and the amount of NADH, the NADH/NAD^+ in the sample can be calculated.

ATP assay:

The determination of ATP is based on the fact that ATP provides energy for firefly luciferase to catalyze luciferin to produce fluorescence. Results are typically recorded using a luminometer. When both the firefly luciferase and luciferin are excessive, the intensity of fluorescence is proportional to the concentration of ATP within a certain concentration range. All reagents are provided by the Kit. All sample preparation and detection were performed under 4°C environmental condition or on an ice bed.

Supplementary Note 2.

The ΔG^0 (kJ/mol) of functional group transformation using eQuilibrator were presented as follows:

Reaction A: pyruvate (-345.8) + CO_2 (-386.0) → oxaloacetate (-714.5) ΔG^0 (A) = +17.3 kJ/mol

Reaction B: oxaloacetate (-714.5) → MSA (-356.6) + CO_2 (-386.0) ΔG^0 (B) = -28.1 kJ/mol

Reaction C: MSA (-356.6) + NADH (-1141.6) → 3-HP (-316.3) + NAD^+ (-1205.8) ΔG^0 (C) = -23.9 kJ/mol

Total $\Delta G^0 = \Delta G^0$ (A) + ΔG^0 (B) + ΔG^0 (C) = -34.7 kJ/mol

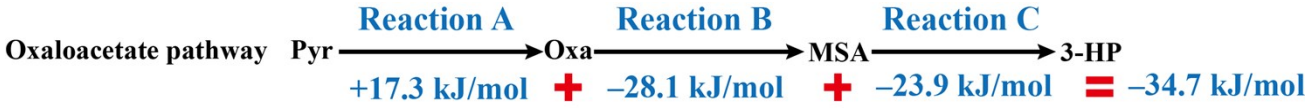

Supplementary Note 3.

The optimal stoichiometry for converting glucose to pyruvate is calculated by equation (1). This indicates that the cytoplasmic energy module generates 2 mol ATP.

$$glucose + 2Pi + 2ADP + 2NAD^+ \rightarrow 2pyruvate + 2ATP + 2NADH + 2H^+ + 2H_2O \quad (1)$$

The optimal stoichiometry for converting pyruvate to 3-HP is calculated by equation (2). This indicates that the 3-HP production module consumes 2 mol ATP.

$$2pyruvate + 2ATP + 2NADH + 2H^+ \rightarrow 2\ 3\text{-}HP + 2ADP + 2Pi + 2NAD^+ \quad (2)$$

Supplementary Note 4.

The optimal stoichiometry after acetyl-coenzyme (CoA) enters the tricarboxylic acid (TCA) cycle is calculated by equation (3). The stoichiometry of ATP generated by NADH and $FADH_2$ produced

by the TCA cycle through the oxidative phosphorylation pathway is calculated by equations (4) and (5), respectively. In summary, the stoichiometry of ATP generated by mitochondria energy module can be calculated by equation (6) = 2 * (3) + 6 * (4) + 2 * (5). This indicates that the mitochondria energy module generates 20 mol ATP.

$$\text{Acetyl-CoA}+3\text{NAD}^{+}+\text{FAD}+\text{ADP(GDP)}+\text{Pi}\rightarrow 2\text{CO}_2+3\text{NADH}+\text{FADH}_2+\text{ATP(GTP)}+2\text{H}^{+}+\text{CoA-SH} \quad (3)$$

$$\text{NADH} + \text{H}^{+} + 2.5\text{ADP} + 2.5\text{Pi} + 1/2\text{O}_2 \rightarrow \text{NAD}^{+} + \text{H}_2\text{O} + 2.5\text{ATP} \quad (4)$$

$$\text{FADH}_2 + 1.5\text{ADP} + 1.5\text{Pi} + 1/2\text{O}_2 \rightarrow \text{FAD} + \text{H}_2\text{O} + 1.5\text{ATP} \quad (5)$$

$$2\text{Acetyl-CoA} + 20\text{ADP} + 20\text{Pi} + 2\text{H}^{+} + 4\text{O}_2 \rightarrow 4\text{CO}_2 + 20\text{ATP} + 8\text{H}_2\text{O} + 2\text{CoA-SH} \quad (6)$$

Supplementary Note 5.

As shown in Supplementary Fig. 3d-f, the intracellular concentration of glucose-6-phosphate (G6P), fructose-6-phosphate (F6P), and phosphoenolpyruvate (PEP) in strain thTAM-23 was higher than that in the control strain thTAM-20 at 24, 48, 72, and 96 h, respectively. The concentration of G6P at 48 h, F6P at 48 h, and PEP at 24 h in strain thTAM-23 increased by 94.7%, 64.3% and 28.2% compared with that in the control strain thTAM-20, respectively. Furthermore, the whole process of glycolysis accumulates pyruvate and generates additional NADH. Pyruvate yield of strain thTAM-23 was 89.7% higher than that of the control strain thTAM-20 at 108 h (Supplementary Fig. 3b). The [NADH/NAD^{+}] of strain thTAM-23 was 31.0%, 26.9%, 32.7%, and 18.1% higher than that of the control strain thTAM-20 at 24, 48, 72, and 96 h, respectively (Supplementary Fig. 3c). These results directly indicated that glycolysis flux was improved through the increase of Hxk2 activity caused by Glc7 dephosphorylation.

Supplementary Experimental 1.

Fluorescence assay

Strains thTAM-34, thTAM-35, and thTAM-36-1 were cultured in 250-mL flasks containing 30 mL YNB media to Mid-log phase, and then inoculate into new YNB media (initial OD_{600nm} = 0.1). To assay cell growth and fluorescence intensity, strain thTAM-34 grown with 0, 100, 200, 300, and 400 μg/mL of phenylalanine (PHE). 0, 1, 2.5, 5, 10, and 25 μmol/L of α-pheromone were respectively added when strain thTAM-35 was growing to the Mid-log phase (at 20 h), and 0, 100, and 200 μg/mL of PHE were respectively added to the media of strain thTAM-36-1 at 12 h. Fluorescence intensity assay data were recorded on a SpectraMax M3 plate reader (Molecular Devices) using 96-well plates. The EGFP intensity was measured at an excitation wavelength of 480 ± 5 nm and an emission wavelength of 515 ± 10 nm. All fluorescence was normalized with cell density by measuring the corresponding absorbance at 600 nm. At the same time, fluorescence microscopy images were obtained with a *Nikon* ECLIPSE 80i microscope equipped with a ×100 oil immersion objective. Brightfield images (exposure, 100 ms) and EGFP fluorescence images (FITC, exposure, 500 ms) were analysed using Image J software. For all microscopy experiments, cell were harvested, washed, and suspended in PBS.

Supplementary Experimental 2.

Hexokinase activity assay

Strains thTAM-24 and thTAM-25 were cultured in YNB medium to exponential-phase. Yeast cell were harvested, washed, resuspended in PBS (pH = 7.4), and subsequently broken by freezingthawing in liquid nitrogen. Cell extracts were prepared for the determination of Hexokinase activity using Hexokinase Colorimetric Assay Kit (Sinobestbio, Shanghai, China). The experimental operation steps were performed according to the instructions. Protein concentrations in cell extracts were determined by the Bradford Protein Assay Kit (Sangon Biotech, Shanghai, China).

Supplementary Experimental 3.

Intracellular concentration of glucose-6-phosphate (G6P), fructose-6-phosphate (F6P), and phosphoenolpyruvate (PEP) assay

Intracellular concentration of glucose-6-phosphate (G6P), fructose-6-phosphate (F6P), and phosphoenolpyruvate (PEP) in strain thTAM-20 and thTAM-23 were determined by the Glucose-6-Phosphate Assay Kit (MAK014), Fructose-6-Phosphate Assay Kit (MAK020), and PEP Colorimetric/Fluorometric Assay Kit (MAK102), respectively. All Assay Kits were purchased from Sigma-Aldrich LLC. Yeast cells were collected and washed (5000 rpm, 5 min) during shake flask fermentation at 24, 48, 72, and 96 h, respectively. Different from the above-mentioned kit operation steps, the cell disruption solution is obtained by liquid nitrogen freeze grinding.

Supplementary Experimental 4.

Oxygen consumption rate measurements

The oxygen consumption rate (OCR) measurements were carried out as described in previous reports with minor modifications. [16] Strains thTAM-30, thTAM-31, thTAM-32, and thTAM-33 were

322 respectively cultured overnight in YNB medium until mid-log phase at 30 °C and diluted to OD_{600} =
323 0.3 in fresh YNB medium. In addition, the final concentrations of oligomycin, FCCP and Rotenone &
324 antimycin A were 15, 5, and 5 μM. The oxygen consumption rate was measured according to the
325 manufacturer's manual on a Seahorse XF96 Extracellular Flux Analyzer (Seahorse Bioscience,
326 Billerica, MA). Three wells were used for each strain.
327
328 **Supplementary Experimental 5.**
329 **Transcriptional analysis**
330 Total RNA was extracted using the RNAprep pure Plant Kit and reverse transcription was carried
331 out according to the Prime-Script® RT reagent kit Perfect Real Time (TaKaRa Biotechnology Co.,
332 Ltd.). Real-time quantitative PCR (qPCR) was designed as described in previous reports. [17]
333
334 **Supplementary Experimental 6.**
335 Branched-chain alpha-keto acid decarboxylase (KdcA, EC:4.1.1.2) and benzoylformate
336 decarboxylase (MdlC, EC:4.1.1.7) activity were measured by coupling the reduction of aldehydes
337 catalyzed by alcohol dehydrogenase and one unit of activity was defined as that the oxidation of 1
338 μmol NADH per minute by measurement of the absorbance at 340 nm. KdcA activity was determined
339 as previously. [18] The corresponding reaction mixture (200 μL, pH = 6.3, 30 °C) containing 50 mM
340 sodium citrate (adjust pH = 6.3 with 1 mol/L HCl), 10 mM thiamine diphosphate (ThDP), 10 mM
341 $MgCl_2$, 10 mM NADH, 5 μL ethanol dehydrogenase, 10 mM oxaloacetate, and 50 μL enzyme solution.
342 MdlC activity was determined according to previously described methods. [19] The corresponding
343 reaction mixture (200 μL, pH = 6.5, 30 °C) containing 100 mM potassium phosphate buffer, 0.3 mM

NADH, 5 μL ethanol dehydrogenase, 2 mM oxaloacetate, 10 mM $MgCl_2$, 10 mM ThDP, and 50 μL enzyme solution. 3-hydroxyisobutyrate dehydrogenases (MmsB, EC:1.1.1.31) was determined according to previously reported methods, [20] with minor modification. The corresponding reaction mixture added 10 mM NADH as cofactor and 1 mM malonate semialdehyde as substrate. Pyc activity was determined as described. [21] Pyc and MmsB activity was defined as described above. All enzyme activities were determined on a SpectraMax M3 microplate reader (Molecular Devices, Sunnyvale, CA).

Supplementary Experimental 7.

Fed-batch fermentation

Strain thTAM-43 was inoculated in 100 mL YNB medium in a 500 mL shake flask and cultured at 30 °C with 200 rpm agitation as seed culture. 0.3 L seed culture was centrifuged and suspended in synthetic medium and then inoculated into the bioreactor. Batch fermentation was carried out in a 5-L bioreactor (BXBIO, Shanghai, China) containing 2.7 L synthetic medium with an initial OD_{600} = 0.3. The working volume was 3.0 liters, and fermentation was performed at 30 °C for 108 h with an agitation speed of 500 rpm and an aeration rate of 1.5 vvm. The culture pH was maintained at 5.0 by automatic addition of 6 M KOH. To induce the QS system, PHE with a final concentration of 100 μg/mL was added to the fermentation broth at 12 h. For fed-batch cultivations, the 20 g/L glucose was added after the glucose was exhausted.

Supplementary Experimental 8.

Isolation of 3-HP from fermentation broth

Isolation of 3-HP from fermentation broth were performed as described in previous patents [22, 23] with appropriate modifications. The steps and parameters were listed below:

(ⅰ) Centrifugation: yeast biomass was removed from the broth using centrifugation (8000 rpm for 5 min) and then the supernatant was decanted.

(ⅱ) Decolorization: the supernatant was decolorized by adding activated carbon particles (carbon granularity 80 mesh, 5 g/L, 30 min) and centrifuged (12000 rpm for 5 min). The supernatant was decanted.

(ⅲ) Acidulation: the protein in the broth was removed by adding concentrated H_2SO_4 until the pH of the broth solution was 1.25. The precipitated protein was removed using centrifugation (12000 rpm for 8 min) and the supernatant was then decanted.

(ⅳ) Ion Exchange: the impurity organic acid in acidulated fermentation broth was removed by weak-base anion exchange. The anion exchange resin is D314 Weak-Base Anion Exchange resin available from the ANHUI SANXING RESIN TECHNOLOGY CO., LTD, CHINA. The glass column (25 mm × 600 mm) was obtained from BEIJING SYNTHWARE GLASS, LTD, CHINA.

Resin pretreatment:

(a) The untreated resin was soaked in a saturated NaCl solution for 2 h and gradually diluted to pure water.

(b) Soak the resin in pure water for 12 h, wait until the resin is fully expanded.

(c) Soak the resin in 5.0 wt % HCl for 4 h and rinse with pure water to pH = 4.0.

(d) Soak the resin in 5.0 wt % NaOH and rinse with pure water until pH =8.5.

Adsorption and elution:

The peristaltic pump controled the injection sample flow rate to 3.0 mL/min. Take 2.0 mol/L NaOH as the eluent, and the flow rate of eluent was 3.0 mL/min.

Resin regeneration

(a) Wash with pure water, then eluted with 5.0 wt % NaOH solution for 2 h.

(b) Eluted with pure water until pH = 8.5.

(v) Distillation: the material was concentrated with a rotary evaporator for vacuum distillation. The temperature was set at 60 °C for 20.0 min.

References

1. C. Rathnasingh, S. M. Raj, Y. Lee, C. Catherine, S. Ashok and S. Park, *J. Biotechnol.*, 2012, **157**, 633-640.
2. C. Liu, Y. Ding, R. Zhang, H. Liu, M. Xian and G. Zhao, *Metab. Eng.*, 2016, **34**, 104-111.
3. Z. Cheng, J. Jiang, H. Wu, Z. Li and Q. Ye, *Bioresour. Technol.*, 2016, **200**, 897-904.
4. M. D. Lynch, R. T. Gill and T. W. Lipscomb, US Pat., US9388419, 2016.
5. B. Liang, G. Sun, Z. Wang, J. Xiao and J. Yang, *Green Chem.*, 2019, **21**, 6103-6115.
6. H. S. Chu, Y. S. Kim, C. M. Lee, J. H. Lee, W. S. Jung, J. H. Ahn, S. H. Song, I. S. Choi and K. M. Cho, *Biotechnol. Bioeng.*, 2015, **112**, 356-364.
7. C. W. Song, J. W. Kim, I. J. Cho and S. Y. Lee, *ACS Synth. Biol.*, 2016, **5**, 1256-1263.
8. Y. Chen, J. Bao, I. K. Kim, V. Siewers and J. Nielsen, *Metab. Eng.*, 2014, **22**, 104-109.
9. X. Chen, X. Yang, Y. Shen, J. Hou and X. Bao, *ACS Synth. Biol.*, 2017, **6**, 905-912.
10. F. David, J. Nielsen and V. Siewers, *ACS Synth. Biol.*, 2016, **5**, 224-233.
11. K. R. Kildegaard, N. B. Jensen, K. Schneider, E. Czarnotta, E. Ozdemir, T. Klein, J. Maury, B. E. Ebert, H. B. Christensen, Y. Chen, I. K. Kim, M. J. Herrgard, L. M. Blank, J. Forster, J. Nielsen and I. Borodina, *Microb. Cell Fact.*, 2016, **15**, 53-65.
12. S. Shi, Y. Chen, V. Siewers and J. Nielsen, *mBio*, 2014, **5**, e01130-01114.
13. I. Borodina, K. R. Kildegaard, N. B. Jensen, T. H. Blicher, J. Maury, S. Sherstyk, K. Schneider, P. Lamosa, M. J. Herrgard, I. Rosenstand, F. Oberg, J. Forster and J. Nielsen, *Metab. Eng.*, 2015, **27**, 57-64.
14. S. Takayama, A. Ozaki, R. Konishi, C. Otomo, M. Kishida, Y. Hirata, T. Matsumoto, T. Tanaka and A. Kondo, *Microb. Cell Fact.*, 2018, **17**, 176.
15. Z. Chen, J. Huang, Y. Wu, W. Wu, Y. Zhang and D. Liu, *Metab. Eng.*, 2017, **39**, 151-158.
16. T. Srikumar, M. C. Lewicki, M. Costanzo, J. M. Tkach, H. van Bakel, K. Tsui, E. S. Johnson, G. W. Brown, B. J. Andrews, C. Boone, G. Giaever, C. Nislow and B. Raught, *J. Cell Biol.*, 2013, **201**, 145-163.
17. X. Chen, G. Xu, N. Xu, W. Zou, P. Zhu, L. Liu and J. Chen, *Metab. Eng.*, 2013, **19**, 10-16.
18. B. A. Smit, J. E. T. van Hylckama Vlieg, W. J. M. Engels, L. Meijer, J. T. M. Wouters and G. Smit, *Appl. Environ. Microbiol.*, 2005, **71**, 303-311.
19. M. B. Marc Bruning, Danilo Meyer, Ralph Golbik, Hans Bartunik, Andreas Liese, Kai Tittmann, *Biochem.*, 2009, **48**,

3258-3268.
20. T. Yao, L. Xu, H. Ying, H. Huang and M. Yan, *Appl. Biochem. Biotechnol.*, 2009, **160**, 694-703.
21. X. Chen, P. Zhu and L. Liu, *Metab. Eng.*, 2016, **33**, 76-85.
22. T. W. Abraham, E. Allen, J. J. Hahn, P. Tsobanakis, E. C. Bohnert and C. L. Frank, US Pat., US10442748B2, 2019.
23. R. Tengler, D. D. Coster, US Pat., US20130345470A1, 2013.